

# Thermochemical and Kinetic Study of the Carbocation Ring Contraction of Cyclohexylium to Methylcyclopentylum

Iain D. Mackie,<sup>‡</sup> Jagannathan Govindhakannan,<sup>†</sup> and Gino A. DiLabio<sup>\*‡</sup>

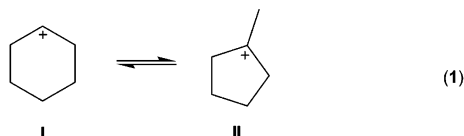
National Institute for Nanotechnology, 11421 Saskatchewan Drive, Edmonton, Alberta, Canada T6G 2M9, and National Centre for Upgrading Technology, Natural Resources Canada, 1 Oil Patch Drive, Devon, Alberta, Canada T9G 1A8

Received: November 6, 2007; In Final Form: February 4, 2008

The isomerization of cyclohexylium to methylcyclopentylum is a model for a key step required in sterol and triterpene biosynthesis and is important in catalytic processes associated with ring-opening reactions in upgrading petroleum fractions. Using high-level, correlated wave function techniques based on QCISD, the mechanism for this isomerization was found to be very different from that first proposed more than 35 years ago. On the basis of our mechanism, a first-order rate constant expression was derived and used with complete basis set-extrapolated QCISD(T) energies to obtain  $E_a = 6.9$  kcal/mol and  $A = 10^{11.18}$  s<sup>-1</sup>, in excellent agreement with values of  $7.4 \pm 1$  kcal/mol and  $A = 10^{12 \pm 1.3}$  s<sup>-1</sup> measured in the gas phase. The B3LYP and MP2 methods, two commonly used computational approaches, were found to predict incorrect mechanisms and, in some cases, poor kinetic parameters. The PBE method, however, produced a reaction profile and kinetic parameters in reasonable agreement with those obtained with the complete basis set-extrapolated QCISD(T) method.

## Introduction

The isomerization of cyclohexylium (**I**) to the 1-methylcyclopentyl cation (**II**) was studied by Olah et al. using NMR.<sup>1</sup> Hydride abstraction from cyclohexane by FSO<sub>3</sub>H–SbF<sub>5</sub> at –60 °C produced 1-methylcyclopentyl cation on a time scale that was too fast to allow observation of the cyclohexyl cation by NMR. Using similar acidic conditions, Saunders and Rosenfeld later obtained an Arrhenius activation energy ( $E_a$ ) of  $18.2 \pm 0.1$  kcal/mol and  $\log(A) = 13.6 \pm 0.1$  for **1**.<sup>2</sup> The rearrangement mechanism was proposed to involve a protonated cyclopropane intermediate, and the results of later semiempirical modeling work by Viruela-Martin et al. were found to be consistent with that mechanism.<sup>3</sup> The first gas-phase study yielding Arrhenius parameters for **1** was conducted by Attinà et al.<sup>4</sup> who measured a substantially smaller  $E_a$  value of  $7.4 \pm 1$  kcal/mol and a lower  $\log(A) = 12 \pm 1.3$ . These findings imply that solvation may have a substantial influence on the kinetics of **1**. The mechanism may also be effected by solvation.



The importance of **1** extends beyond that associated with a prototypical carbocation rearrangement. Reaction **1** (or, more accurately, the reverse of **1**) is a model for a key step in the enzymatic cyclization required in sterol and triterpene biosynthesis.<sup>5</sup> Not surprisingly, these rearrangements have been the

subject of several simulation studies involving the use of semiempirical,<sup>6</sup> Hartree–Fock, and density functional theory (DFT).<sup>7</sup> Most recently, Vrček et al. used Møller–Plesset techniques to determine the reaction profile for the rearrangement of the 1-(2-propyl)cyclopentyl cation to the 1,2-dimethyl-1-cyclohexyl cation.<sup>8</sup> Their findings were in agreement with the large  $E_a$  reported for **1** by Saunders and Rosenfeld.<sup>2</sup>

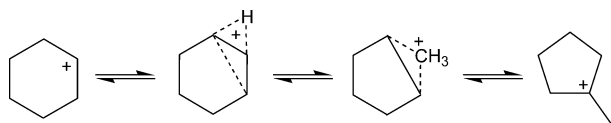
Reaction **1** is significant in understanding ring-opening reactions in the upgrading of petroleum fractions. Insights into the details of **1** will help to understand ring-opening processes in naphthenes containing two or more rings. The hydrogenation of aromatic compounds yields a minor improvement to the cetane number of fuel constituents. However, the ring-opening of these compounds can lead to very large increases in cetane number.<sup>9</sup> The catalysis of the cracking of cyclohexane using acidic zeolites is therefore important. The cyclohexylium intermediates formed during the catalytic processes can undergo isomerization to methylcyclopentylum, a process that may facilitate ring-opening. In the context of C6 cyclization, Thomson's group has studied **1** in the gas phase<sup>10</sup> and on zeolite models<sup>11</sup> using DFT. They computed that **1** has an energy barrier of 9.6 kcal/mol,<sup>10,12</sup> substantially lower than the value reported in ref 2 and close to that obtained from the gas-phase measurements of Attinà et al.<sup>4</sup>

We are motivated to understand the details of the thermochemistry and kinetics of **1** by its importance in biochemistry and petroleum refining and by the apparent discrepancies between reported experimental and calculated activation energies. In this work, we apply high-level wave function techniques to elucidate the reaction profile and thermochemistry of **1**. The data are then used together with a derived kinetics expression to arrive at Arrhenius parameters for **1**. The results reported herein will serve as a benchmark for future simulation work involving cyclic carbocation rearrangements.

\* To whom correspondence should be addressed. Phone: +1-780-641-1729. E-mail: Gino.DiLabio@nrc.ca.

<sup>‡</sup> National Institute for Nanotechnology.

<sup>†</sup> National Centre for Upgrading Technology.

**SCHEME 1: Reaction Mechanism for 1, Originally Proposed in Reference 13****Mechanism of 1**

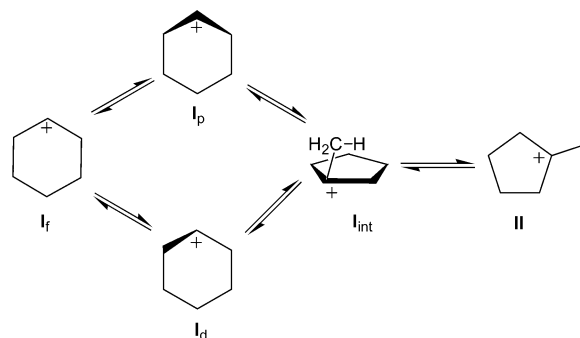
The mechanism of **1**, originally proposed by Nenitzescu<sup>13</sup> and supported by Olah et al.,<sup>1</sup> is illustrated in Scheme 1. The rearrangement was thought to involve a protonated cyclopropane intermediate and avoids the formation of primary carbocations during the reaction. Later semiempirical modeling by Viruela-Martin et al. supported the proposal that the first intermediate is an edge-protonated bicyclic species.<sup>3</sup> However, the modeling predicted the formation of a secondary methylcyclopentylum cation as the second intermediate, via a protonated cyclopropane transition-state (TS) structure, prior to conversion to **II**. A second, higher-energy reaction path connecting the first and second intermediates was also identified.<sup>3</sup>

More recent DFT work by Joshi et al.<sup>14</sup> suggests that the mechanism of **1** is somewhat more complicated than earlier proposals.<sup>10</sup> They found three low-energy conformations for **I**. One of these structures was found to directly form a secondary methylcyclopentylum cation through a cyclopropane transition state structure. The secondary cation was predicted to convert directly to **II** without passing through a TS. This pathway is similar to the low-energy pathway predicted by Viruela-Martin et al.<sup>3</sup> A second structure for **I** was predicted to convert to **II** by a high-energy pathway through a TS structure with substantial primary carbocationic character.

In our own initial attempts to establish the reaction profile of **1**, we used B3LYP<sup>15</sup> (a hybrid DFT method) and MP2 (a correlated wave function method) with 6-31G(d) basis sets.<sup>16</sup> Immediately obvious from the preliminary work was that the pathways of **1** that are predicted by theory are highly sensitive to the methods employed. Additional calculations performed with larger basis sets (6-31+G(d,p), 6-311++G(d,p), 6-311++G-(2d,2p)) revealed that the predictions for reaction pathways are also basis set dependent, as are the relative energies of the intermediate and TS structures of those pathways. The reader is directed toward the Supporting Information (SI) for specific examples of the failures of these methods with smaller basis sets.

It was clear from our initial test calculations that we needed to resort to higher-level theory to resolve the reaction pathways of **1**. For this, we chose to use the QCISD method with 6-311++G(d,p) basis sets. The QCISD approach has been shown by others to predict accurate geometries and energies for TS structures for open-shell systems.<sup>17</sup> Our own tests give us confidence that the reaction pathways and structures we computed using this approach are well converged with the selected basis sets.<sup>18</sup> However, the relative energies of points along the reaction profile converge more slowly than do the geometries, and we required more extensive treatments of correlation. We therefore performed calculations to estimate the QCISD(T) energies at the complete basis set (CBS) limit<sup>19</sup> of the QCISD/6-311++G(d,p)-optimized structures (QCISD(T)/CBS(QCISD)//QCISD/6-311++G(d,p)).<sup>22</sup>

Our proposed mechanism for **1** is shown in Scheme 2, and the structural details of the stationary points along the reaction path are provided in SI. Figures 2 and 3 illustrate some of the structures associated with **1**. Table 1 contains and Figure 1

**SCHEME 2: QCISD(T)/CBS(QCISD)//QCISD/6-311++G(d,p) Reaction Mechanism for 1**

illustrates the relative energies of the stationary points for that mechanism. In the experimental study of the thermal isomerization of **I**,<sup>4</sup> the cation is produced via hydride-ion abstraction from cyclohexane. Abstraction of a hydride from either an axial or an equatorial position leads to structures of **I** that are either flat (**I<sub>f</sub>**) or puckered (**I<sub>p</sub>**) about the charge center (see Figure 2). A third isomer also exists in which the CH<sub>2</sub>  $\alpha$  to the charge center lies out of the plane of the ring. We label this distorted structure as **I<sub>d</sub>** (see Figure 2). Both **I<sub>p</sub>** and **I<sub>d</sub>** are energetically more stable than **I<sub>f</sub>** by  $\sim 3.4$  and  $1.1$  kcal/mol, respectively. As can be seen in Figure 1, the calculations show that the three **I** structures are able to easily interconvert. The TS structures connecting **I<sub>f</sub>** to **I<sub>p</sub>** and to **I<sub>d</sub>** (TS<sub>I<sub>f</sub>-I<sub>p</sub></sub> and TS<sub>I<sub>f</sub>-I<sub>d</sub></sub>) are 2.4 and 3.0 kcal/mol, respectively, higher in energy than that of **I<sub>f</sub>**. The TS structure connecting **I<sub>p</sub>** and **I<sub>d</sub>** (TS<sub>I<sub>p</sub>-I<sub>d</sub></sub>) is 1.5 kcal/mol higher in energy than **I<sub>f</sub>**. These TS structures are shown in Figure 3.

From cyclohexylium, the reaction proceeds to an intermediate structure, **I<sub>int</sub>**, via two pathways, with TS structures that are formed by ring contractions and hydrogen transfers between ring carbons. **I<sub>f</sub>** cannot directly convert to **I<sub>int</sub>** but must first convert to **I<sub>p</sub>** or **I<sub>d</sub>**. **I<sub>d</sub>** converts to **I<sub>int</sub>** via TS<sub>I<sub>d</sub>-I<sub>int</sub></sub>, and **I<sub>p</sub>** converts to **I<sub>int</sub>** via TS<sub>I<sub>p</sub>-I<sub>int</sub></sub>. The main difference between these structures is whether the out-of-plane ring methyl group is puckered above or below the plane of the pentyl ring relative to the migrating hydrogen (see Figure 3). Despite the similarities, however, steric repulsions between the out-of-plane methyl and above-plane pentyl ring hydrogens in TS<sub>I<sub>p</sub>-I<sub>int</sub></sub> cause it to be higher in energy than TS<sub>I<sub>d</sub>-I<sub>int</sub></sub> by 3.3 kcal/mol. The barriers to conversion to **I<sub>int</sub>**

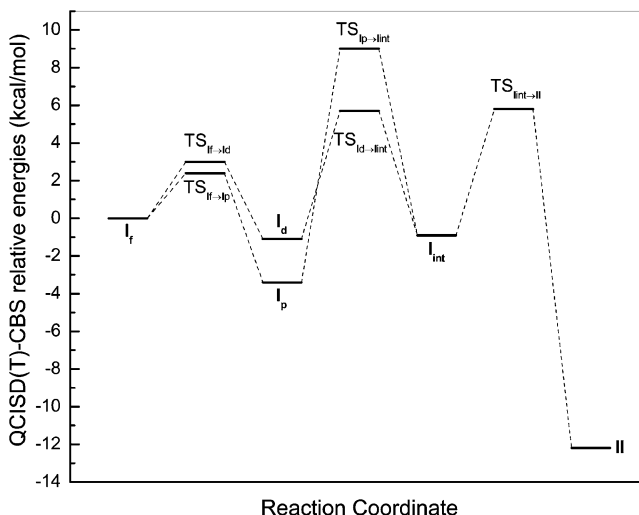


**Figure 1.** Relative energies of stationary points along the QCISD(T)/CBS(QCISD)//QCISD/6-311++G(d,p) reaction profile.

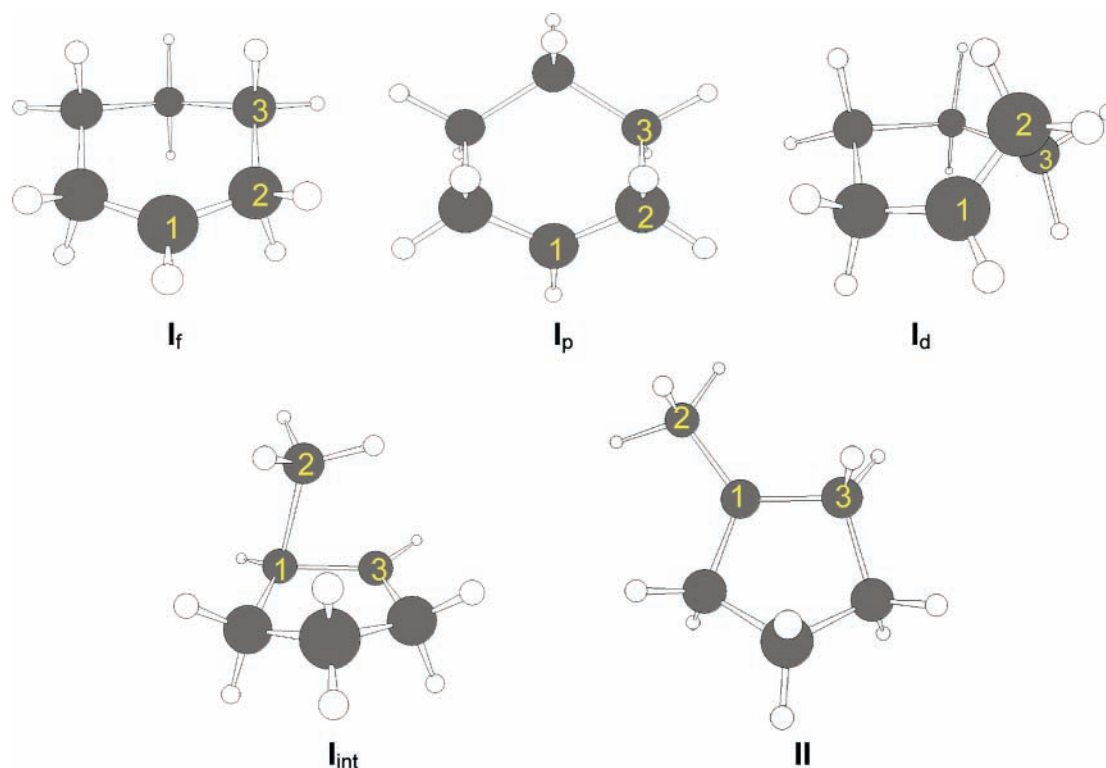


**Figure 2.** Optimized structures associated with the minima along the reaction profile of **1**; see Scheme 2.

are predicted to be much larger for the lowest-energy cyclohexylium structure, **I<sub>p</sub>** (12.4 kcal/mol), compared to **I<sub>d</sub>** (6.8 kcal/mol). Nevertheless, both pathways will contribute to the kinetics of **1** because this barrier height difference will be offset by the larger (Boltzmann) population of **I<sub>p</sub>** relative to that of **I<sub>d</sub>**.

Our calculations predict **I<sub>int</sub>** to have an asymmetric structure with a CH<sub>3</sub> group above and closer to one side of an incipient  $\pi$ -bond of the cyclopentene-like ring (see Figure 2). The CH<sub>3</sub> group has one hydrogen interacting strongly with a ring carbon and is on the same side of the ring as the puckered CH<sub>2</sub> group. Analysis of the charge distribution indicates that the positive charge is largely centered on the tertiary carbon. This structure of **I<sub>int</sub>** is 0.9 kcal/mol lower in energy than **I<sub>f</sub>**.

In the final step of the rearrangement, **I<sub>int</sub>** converts to **II** via TS<sub>**I<sub>int</sub>**→**II**</sub>. This TS structure resembles a secondary methylcyclopentylum carbocation, with the charge residing on the ring carbon in the  $\alpha$ -position relative to that of the exocyclic methyl group; see Figure 3. The energy barrier of the last step in **1** is calculated to be 6.7 kcal/mol higher than that for **I<sub>int</sub>**. The overall rearrangement is predicted to be -12.2 kcal/mol exoergic.

### Kinetics of **1**

On the basis of our calculated mechanism (Scheme 2), we were able to derive an expression for the rate constant for **1**. Using a quasi-steady-state approximation, we determined the rate constant expression for the forward reaction,  $k_1$ , to be

$$k_1 = \frac{k_{\mathbf{I}_{\text{int}} \rightarrow \mathbf{II}}(d_4 + d_5 K_{\text{fp}})}{1 + K_{\text{fp}}} \quad (\text{a})$$

where

$$d_4 = \frac{\frac{k_{\mathbf{I}_f \rightarrow \mathbf{I}_d}}{k_{\mathbf{I}_d \rightarrow \mathbf{I}_f} + k_{\mathbf{I}_d \rightarrow \mathbf{I}_p} + k_{\mathbf{I}_d \rightarrow \mathbf{I}_{\text{int}}}} \cdot \frac{k_{\mathbf{I}_d \rightarrow \mathbf{I}_{\text{int}}}}{k_{\mathbf{I}_{\text{int}} \rightarrow \mathbf{I}_p} + k_{\mathbf{I}_{\text{int}} \rightarrow \mathbf{I}_d} + k_{\mathbf{I}_{\text{int}} \rightarrow \mathbf{II}}}}{1 - \frac{k_{\mathbf{I}_{\text{int}} \rightarrow \mathbf{I}_d}}{k_{\mathbf{I}_d \rightarrow \mathbf{I}_f} + k_{\mathbf{I}_d \rightarrow \mathbf{I}_p} + k_{\mathbf{I}_d \rightarrow \mathbf{I}_{\text{int}}}} \cdot \frac{k_{\mathbf{I}_d \rightarrow \mathbf{I}_{\text{int}}}}{k_{\mathbf{I}_{\text{int}} \rightarrow \mathbf{I}_p} + k_{\mathbf{I}_{\text{int}} \rightarrow \mathbf{I}_d} + k_{\mathbf{I}_{\text{int}} \rightarrow \mathbf{II}}}}$$

$$d_5 = \frac{\frac{k_{\mathbf{I}_p \rightarrow \mathbf{I}_{\text{int}}}}{k_{\mathbf{I}_{\text{int}} \rightarrow \mathbf{I}_p} + k_{\mathbf{I}_{\text{int}} \rightarrow \mathbf{I}_d} + k_{\mathbf{I}_{\text{int}} \rightarrow \mathbf{II}}} + \frac{k_{\mathbf{I}_f \rightarrow \mathbf{I}_d}}{k_{\mathbf{I}_d \rightarrow \mathbf{I}_f} + k_{\mathbf{I}_d \rightarrow \mathbf{I}_p} + k_{\mathbf{I}_d \rightarrow \mathbf{I}_{\text{int}}}} \cdot \frac{k_{\mathbf{I}_d \rightarrow \mathbf{I}_{\text{int}}}}{k_{\mathbf{I}_{\text{int}} \rightarrow \mathbf{I}_p} + k_{\mathbf{I}_{\text{int}} \rightarrow \mathbf{I}_d} + k_{\mathbf{I}_{\text{int}} \rightarrow \mathbf{II}}}}{1 - \frac{k_{\mathbf{I}_{\text{int}} \rightarrow \mathbf{I}_d}}{k_{\mathbf{I}_d \rightarrow \mathbf{I}_f} + k_{\mathbf{I}_d \rightarrow \mathbf{I}_p} + k_{\mathbf{I}_d \rightarrow \mathbf{I}_{\text{int}}}} \cdot \frac{k_{\mathbf{I}_d \rightarrow \mathbf{I}_{\text{int}}}}{k_{\mathbf{I}_{\text{int}} \rightarrow \mathbf{I}_p} + k_{\mathbf{I}_{\text{int}} \rightarrow \mathbf{I}_d} + k_{\mathbf{I}_{\text{int}} \rightarrow \mathbf{II}}}}$$

and  $K_{\text{fp}} = k_{\mathbf{I}_f \rightarrow \mathbf{I}_p}/k_{\mathbf{I}_p \rightarrow \mathbf{I}_f}$ . The details of the derivation of eq 4 are given in the SI. Using QCISD(T)/CBS(QCISD)//QCISD/6-311++G(d,p) energies corrected for zero-point vibration energies and calculated partition functions, we calculated  $k_1$  over a number of temperatures. These were used to obtain an Arrhenius activation energy,  $E_a = 6.9$  kcal/mol, and a pre-exponential factor,  $A = 10^{11.18} \text{ s}^{-1}$ , for **1**. These data compare extremely well with those measured by Attinà et al., namely,  $7.4 \pm 1$  kcal/mol and  $A = 10^{12 \pm 1.3} \text{ s}^{-1}$ .<sup>4</sup>

### Performance of Other Theoretical Approaches

We have a high degree of confidence in the thermochemical and kinetic predictions made by QCISD(T)/CBS(QCISD)//QCISD/6-311++G(d,p) for **1**. As such, we are able to assess the other theoretical approaches used during our preliminary investigations for the mechanism of **1** against our high-level

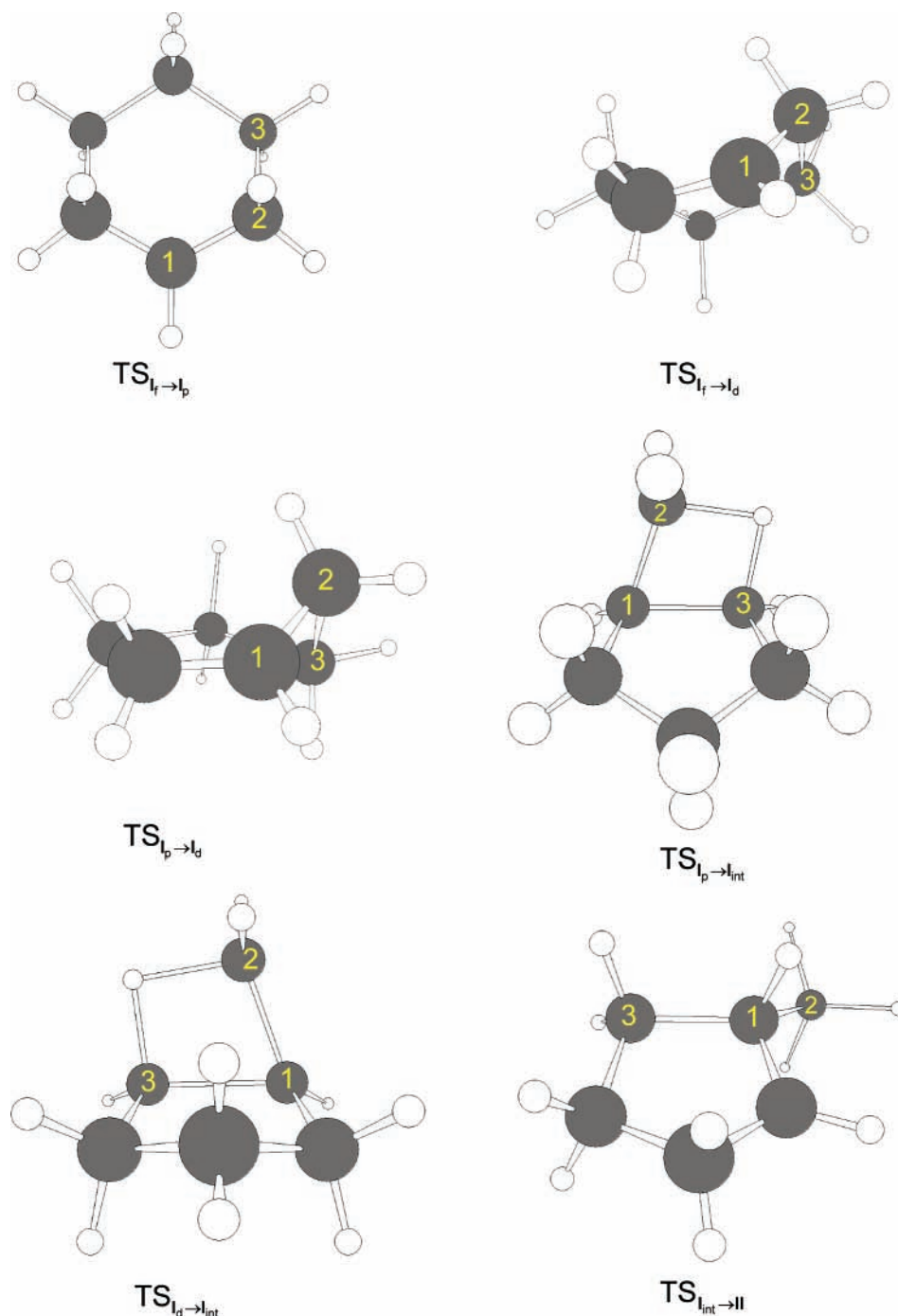


**Figure 3.** Optimized transition-state structures associated with the interconversion of the minimum-energy structures (illustrated in Figure 2) for **1**.

results. We are particularly interested in the performance of the B3LYP functional because it is commonly applied and the MP2 wave function approach because it is often used as a check of results obtained by DFT methods. We are also interested in the PBE functional<sup>23</sup> because it has been implemented in programs that incorporate periodic boundary conditions,<sup>24</sup> which may be useful for studying **1** in a zeolite environment. We relegate most of the large body of data that we computed for **1** using these various methods to the SI and discuss only those points that are relevant to accurate predictions associated with the mechanism and energies. All of the results discussed in this section were obtained using 6-311++G(2d,2p) basis sets, which are large enough to ensure that all structures are converged with respect to basis set size while also being of practical size.<sup>25</sup> We also computed QCISD(T)/CBS(MP2) energies<sup>26</sup> for structures

obtained using the theoretical approaches (i.e., QCISD(T)/CBS(MP2)//method, where method represents the technique used for geometry optimization). These energy data are useful because when compared to QCISD(T)/CBS(MP2)//QCISD/6-311++G(d,p) energies, they provide a single metric for assessing the quality of a predicted structure against those obtained by using QCISD/6-311++G(d,p). Relative energies using QCISD(T), MP2, B3LYP, and PBE for the structures along the reaction profile of **1** are collected in Table 1. Kinetic data obtained using eq a and the energies from the various methods are presented in Table 2.

**MP2.** The MP2 approach performs rather poorly for several points along the reaction profile of **1**. With the exception of two structures, the relative energies predicted with MP2/6-311++G(2d,2p) agree with those obtained with QCISD(T)/

**TABLE 1: Relative (to  $I_f$ ) Energies (kcal/mol) for Optimized Structures Calculated by QCISD(T)/CBS(QCISD)//QCISD/6-311++G(d,p), MP2, B3LYP, and PBE**

structure	QCISD(T) <sup>a</sup>	MP2 <sup>b</sup>	B3LYP <sup>b</sup>	PBE <sup>b</sup>
TS <sub>I<sub>f</sub>→I<sub>p</sub></sub>	+2.4	+2.2	+2.4	+3.0
I <sub>p</sub>	-3.4	-5.2	-1.6	-1.4
TS <sub>I<sub>f</sub>→I<sub>d</sub></sub>	+3.0	+2.6	+3.2	+3.0
I <sub>d</sub>	-1.1	-3.5	+2.3	+1.5
TS <sub>I<sub>p</sub>→I<sub>d</sub></sub>	+1.5	-0.7	+4.2	+3.5
TS <sub>I<sub>p</sub>→I<sub>int</sub></sub>	+9.0	+6.5	+15.2	+11.3
TS <sub>I<sub>d</sub>→I<sub>int</sub></sub>	+5.7	+2.7	+12.0	+8.1
I <sub>int</sub>	-0.9	-4.2	+2.4	+1.7
TS <sub>I<sub>int</sub>→II</sub>	+5.8	-0.3	+5.2	+5.5
II	-12.2	-12.8	-12.4	-12.2

<sup>a</sup> QCISD(T)/CBS(QCISD) energies obtained for the QCISD/6-311++G(d,p)-optimized geometries. <sup>b</sup> Using 6-311++G(2d,2p) basis sets.

**TABLE 2: Calculated Arrhenius Parameters for **1** Based on the Mechanism Shown in Scheme 2; Arrhenius Activation Energies,  $E_a$  (kcal/mol), and Pre-exponential Factors,  $\text{Log}(A)$  ( $\log(\text{s}^{-1})$ )**

	$E_a$	$A$
QCISD(T) <sup>a</sup>	6.9	11.18
MP2	7.6	12.49
B3LYP	11.4	11.24
PBE	7.7	11.10
experiment <sup>b</sup>	$7.4 \pm 1$	$12 \pm 1.3$

<sup>a</sup> QCISD(T)/CBS(QCISD)//QCISD/6-311++G(d,p). <sup>b</sup> Ref 4.

CBS(QCISD) to within  $\sim 3.0$  kcal/mol. MP2 erroneously predicts the  $C_s$  symmetric form of **I<sub>p</sub>** to be a transition state. The distorted versions of this isomer are 0.04 kcal/mol lower in energy at the MP2 level. The bonds C(2)–C(3) and C(5)–C(6) have a difference of 0.11 Å with MP2/6-311++G(2d,2p) compared to the QCISD-optimized structure. This distortion is maintained when the aug-cc-pVTZ basis set is employed. The distortion is not determined by any other method or, for that matter, with MP2 and smaller basis sets and would appear to be an artifact of MP2.

The MP2 method incorrectly predicts **I<sub>int</sub>** to have a symmetric, bicyclic structure; see Figure 4a. The overstabilization of charged, bridged intermediates is a recognized shortcoming of MP2<sup>27</sup> and results in the incorrect **I<sub>int</sub>** structure being  $\sim 2.7$  kcal/mol too low in energy. However, the QCISD(T)/CBS(MP2) method, using either QCISD or MP2 geometries, predicts the symmetric bridged structure to be fairly close in energy to the asymmetric **I<sub>int</sub>**. This indicates that the potential connecting the two structures is fairly flat and that the erroneous structural

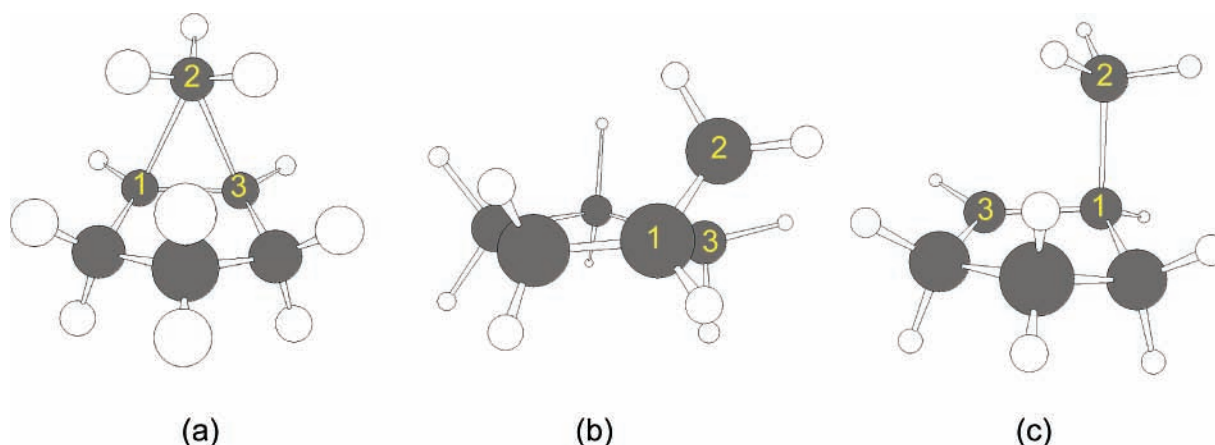
prediction made by MP2 will not greatly effect relative energetics provided that QCISD(T)/CBS(MP2) (or some suitable, high-level alternative) is employed.

The MP2-predicted structure of TS<sub>I<sub>int</sub>→II</sub> closely resembles that obtained using QCISD. However, the relative energy of TS<sub>I<sub>int</sub>→II</sub> is  $\sim 6.1$  kcal/mol lower in energy than that determined by QCISD(T)/CBS(QCISD). This implies that MP2 overstabilizes secondary carbocations. This overstabilization does not have a pronounced effect on structure, and the relative energies determined using QCISD(T)/CBS(MP2) with either QCISD or MP2 geometries are within 0.2 kcal/mol.

Although the QCISD(T)/CBS(QCISD)//QCISD/6-311++G(d,p) and MP2/6-311++G(2d,2p) relative energies for TS<sub>I<sub>f</sub>→I<sub>d</sub></sub> are similar, the predicted structures are noticeably different (cf. Figures 4a and 2). Specifically, the MP2 TS structure has a more pronounced cation- $\pi$ -type bridging interaction than does the QCISD structure. This results in a C(1)–C(2)–C(3) angle in the TS structure that is  $30^\circ$  smaller than that predicted by QCISD. The effect of this overly stable bridging interaction can be recognized in a 1.9 kcal/mol difference in QCISD(T)/CBS(MP2) energies of the QCISD and MP2 structures of TS<sub>I<sub>f</sub>→I<sub>d</sub></sub>. With the exception of TS<sub>I<sub>f</sub>→I<sub>d</sub></sub>, all of the MP2 structures have QCISD(T)/CBS(MP2) relative energies that lie within 0.4 kcal/mol of those of the QCISD-optimized structures.

The kinetic parameters determined by MP2 ( $E_a = 7.6$  kcal/mol,  $A = 10^{12.49} \text{ s}^{-1}$ ; see Table 2) do show moderate agreement with our benchmark data and excellent agreement with Attinà et al.'s measured values. This concurrence reflects the fact that MP2 predicts barrier heights for the individual steps in **1** in close agreement to those obtained by QCISD(T)/CBS(QCISD)//QCISD/6-311++G(d,p), despite the fact that some MP2 relative energies are poorly predicted. We may therefore conclude that the agreement between the kinetic parameters calculated by MP2 and QCISD(T) is fortuitous.

**B3LYP.** Overall, the B3LYP method displays even worse performance than MP2 for the reaction profile for **1**, with several large errors in relative energies ( $> 3$  kcal/mol). Particularly problematic are TS<sub>I<sub>p</sub>→I<sub>int</sub></sub> and TS<sub>I<sub>d</sub>→I<sub>int</sub></sub>, for which the errors in the relative energies are 6.2 and 6.3 kcal/mol, respectively. Interestingly, the B3LYP-optimized TS<sub>I<sub>p</sub>→I<sub>int</sub></sub> and TS<sub>I<sub>d</sub>→I<sub>int</sub></sub> structures compare quite well with the corresponding QCISD TSs, and this is verified by the small differences in the QCISD(T)/CBS(MP2) relative energies obtained for both sets of structures ( $\leq 0.4$  kcal/mol). Additional tests with BHandHLYP and BLYP produce similar results, whereas B3P86 and PBE predict relative energies that are in accord with the QCISD results (see Supporting Information). These findings suggest that the LYP

**Figure 4.** Selected structures erroneously predicted by other theoretical approaches. (a) **I<sub>int</sub>** (MP2), (b) TS<sub>I<sub>f</sub>→I<sub>d</sub></sub> (MP2), (c) **I<sub>int</sub>** (MP2).

correlation functional may be responsible for the poorly predicted energies for  $\text{TS}_{\text{I}_p \rightarrow \text{I}_{\text{int}}}$  and  $\text{TS}_{\text{I}_d \rightarrow \text{I}_{\text{int}}}$ .

B3LYP also predicts an incorrect structure for  $\text{I}_{\text{int}}$ , in which there is no interaction between a hydrogen atom of the exocyclic  $\text{CH}_3$  group and a ring carbon; see Figure 4c. The orientation of the  $\text{CH}_3$  group in the B3LYP structure suggests that  $\text{I}_{\text{int}}$  is a secondary carbocation, and this is confirmed by charge analysis.

Despite the short-comings of B3LYP, all of the predicted structures produce reasonable relative energies at the QCISD(T)/CBS(MP2) level of theory. As expected, the largest error (1.1 kcal/mol) occurs for  $\text{I}_{\text{int}}$ .

B3LYP performs very poorly for the activation energy of **1** ( $E_a = 11.4$  kcal/mol) but satisfactorily for the pre-exponential factor ( $A = 10^{11.24} \text{ s}^{-1}$ ); see Table 2. The large value of  $E_a$  is certainly due to the very high energies associated with the  $\text{I}_p \rightarrow \text{I}_{\text{int}}$  and  $\text{I}_d \rightarrow \text{I}_{\text{int}}$  steps; see Table 1.

**PBE.** The structural predictions made by the PBE functional are in good agreement with the QCISD geometries. We specifically note that the structures for  $\text{I}_{\text{int}}$  (incorrect by MP2 and B3LYP) and  $\text{TS}_{\text{I}_p \rightarrow \text{I}_d}$  (incorrect by MP2) are well-predicted by PBE. However, the PBE relative energies along the reaction coordinate have some fairly large errors. The average of the deviations in the energies relative to the benchmark calculations are the lowest of the three methods tested, namely, MP2 2.3, B3LYP 2.5, and PBE 1.5 kcal/mol.

The  $E_a$  and  $A$  values predicted by PBE are 7.7 kcal/mol and  $A = 10^{11.10} \text{ s}^{-1}$ , respectively, in moderate agreement with the benchmark data and very good agreement with the experimental data.

## Conclusions

The isomerization of the cyclohexylium carbocation to the methylcyclopentylum carbocation is a model for a key step required in sterol and triterpene biosynthesis and is important in catalytic processes associated with upgrading of petroleum fractions. Using high-level, correlated wave function techniques, namely, QCISD/6-311++G(d,p), we determined the gas-phase mechanism for this isomerization. On the basis of our mechanism, a rate constant expression was derived and used, along with QCISD(T) energies extrapolated to the basis set limit, to obtain  $E_a = 6.9$  kcal/mol and  $A = 10^{11.18} \text{ s}^{-1}$ . The calculated kinetic parameters are in excellent agreement with values of  $7.4 \pm 1$  kcal/mol and  $A = 10^{12 \pm 1.3} \text{ s}^{-1}$  measured in the gas phase by Attinà et al.<sup>4</sup>

Using our high-level results as a benchmark, we compared the performance of B3LYP and PBE, two commonly used density functional theory methods, and MP2, a low-cost wave function approach, with respect to the isomerization of cyclohexylium. Our results indicate that, of these methods, only PBE is able to predict the correct reaction profile for the isomerization. Both B3LYP and MP2 produce structures that are not in accordance with those obtained using high-level theory. Therefore, conclusions based on results obtained using B3LYP and MP2 for rearrangements of this type should be treated with caution.

**Acknowledgment.** The authors thank the Canadian Program for Energy Research and Development (PERD) for funding. We are also grateful to the Centre of Excellence for Integrated Nanotools (CEIN) and Academic Information and Communication Technologies (AICT) at the University of Alberta, West-Grid, and Prof. P. Boulanger for providing access to computing resources.

**Supporting Information Available:** Structure coordinates, calculated energies, and details of the kinetic modeling. This material is available free of charge via the Internet at <http://pubs.acs.org>.

## References and Notes

- (1) Olah, G. A.; Bollinger, J. M.; Cupas, C. A.; Lukas, J. *J. Am. Chem. Soc.* **1967**, *89*, 2692–2694.
- (2) Saunders, M.; Rosenfeld, J. *J. Am. Chem. Soc.* **1969**, *91*, 7756–7758.
- (3) Viruela-Martin, P. M.; Nebot, I.; Viruela-Martin, R.; Planelles, J. *J. Chem. Soc. Perkin Trans. 2* **1986**, 49–53.
- (4) Attinà, M.; Cacace, F.; di Marzio, A. *J. Am. Chem. Soc.* **1989**, *111*, 6004–6008.
- (5) See, for example: Abe, I.; Rohmer, M.; Prestwich, G. D. *Chem. Rev.* **1993**, *93*, 2189–2206.
- (6) Rajamani, R.; Gao, J. *J. Am. Chem. Soc.* **2003**, *125*, 12768–12781.
- (7) Jensen, C.; Jorgensen, W. L. *J. Am. Chem. Soc.* **1997**, *119*, 10846–10854.
- (8) Vrček, V.; Saunders, M.; Kronja, O. *J. Org. Chem.* **2003**, *68*, 1859–1866.
- (9) Murphy, M. J.; Taylor, J. D.; McCormick, R. L. Compendium of Experimental Cetane Number Data. <http://www.nrel.gov/vehiclesandfuels/pdfs/sr368051.pdf> (September 2004).
- (10) Joshi, Y. V.; Bhan, A.; Thomson, K. T. *J. Phys. Chem. B* **2004**, *108*, 971–980.
- (11) Joshi, Y. V.; Thomson, K. T. *J. Catal.* **2005**, *230*, 440–463.
- (12) The barrier reported in ref 10 does not include corrections for zero-point vibration energy or enthalpy.
- (13) Nenitzescu, C. D. In *Carbonium Ions*; Olah, G. A., Schleyer, P. v. R., Eds.; Interscience Publishers, Inc.: New York, 1970; p 501.
- (14) Vrček et al.<sup>8</sup> also studied several ring expansion pathways. However, as was pointed out,<sup>10</sup> their work predicts mechanisms that differ substantially from those for **1**. This is because the isopropyl substituents on the cyclopentyl ring model system studied in ref 8 allow for the formation of different tertiary and secondary carbocation intermediates than is possible in **1**.
- (15) (a) Becke, A. D. *J. Chem. Phys.* **1993**, *98*, 5648–5652. (b) Lee, C.; Yang, W.; Parr, R. G. *Phys. Rev. B* **1988**, *37*, 785–789, as implemented in ref 16.
- (16) These calculations were performed using the Gaussian-03 package of programs: Frisch, M. J.; Trucks, G. W.; Schlegel, H. B.; Scuseria, G. E.; Robb, M. A.; Cheeseman, J. R.; Montgomery, J. A., Jr.; Vreven, T.; Kudin, K. N.; Burant, J. C.; Millam, J. M.; Iyengar, S. S.; Tomasi, J.; Barone, V.; Mennucci, B.; Cossi, M.; Scalmani, G.; Rega, N.; Petersson, G. A.; Nakatsuji, H.; Hada, M.; Ehara, M.; Toyota, K.; Fukuda, R.; Hasegawa, J.; Ishida, M.; Nakajima, T.; Honda, Y.; Kitao, O.; Nakai, H.; Klene, M.; Li, X.; Knox, J. E.; Hratchian, H. P.; Cross, J. B.; Bakken, V.; Adamo, C.; Jaramillo, J.; Gomperts, R.; Stratmann, R. E.; Yazyev, O.; Austin, A. J.; Cammi, R.; Pomelli, C.; Ochterski, J. W.; Ayala, P. Y.; Morokuma, K.; Voth, G. A.; Salvador, P.; Dannenberg, J. J.; Zakrzewski, V. G.; Dapprich, S.; Daniels, A. D.; Strain, M. C.; Farkas, O.; Malick, D. K.; Rabuck, A. D.; Raghavachari, K.; Foresman, J. B.; Ortiz, J. V.; Cui, Q.; Baboul, A. G.; Clifford, S.; Cioslowski, J.; Stefanov, B. B.; Liu, G.; Liashenko, A.; Piskorz, P.; Komaromi, I.; Martin, R. L.; Fox, D. J.; Keith, T.; Al-Laham, M. A.; Peng, C. Y.; Nanayakkara, A.; Challacombe, M.; Gill, P. M. W.; Johnson, B.; Chen, W.; Wong, M. W.; Gonzalez, C.; Pople, J. A. *Gaussian 03*, revision C.02; Gaussian, Inc.: Wallingford, CT, 2004.
- (17) Chuang, Y.-Y.; Coitiño, E. L.; Truhlar, D. G. *J. Phys. Chem. A* **2000**, *104*, 446–450.
- (18) One exception is that a structure for  $\text{I}_p$  was predicted to be an intermediate by MP2/6-311+G(d,p) but a TS with MP2/6-311++G(2d,2p). The structures are separated by 0.04 kcal/mol at these two levels of treatment.
- (19) A two-point extrapolation<sup>20</sup> was employed to determine the QCISD(T)/CBS energies. The procedure involves correcting the QCISD(T)/aug-cc-pVDZ energies by the correlation energy calculated from extrapolating QCISD/aug-cc-pVDZ and QCISD/aug-cc-pV TZ energies. The Molpro package of programs was used for these calculations.<sup>21</sup>
- (20) Martin, J. M. L. *Chem. Phys. Lett.* **1996**, *259*, 669–678.
- (21) *MOLPRO*, version 2006.1, a package of ab initio programs; Werner, H.-J.; Knowles, P. J.; Lindh, R.; Manby, F. R.; Schütz, M.; Celani, P.; Korona, T.; Rauhut, G.; Amos, R. D.; Bernhardsson, A.; Berning, A.; Cooper, D. L.; Deegan, M. J. O.; Dobson, A. J.; Eckert, F.; Hampel, C.; Hettler, G.; Lloyd, A. W.; McNicholas, S. J.; Meyer, W.; Mura, M. E.; Nicklass, A.; Palmieri, P.; Pitzer, R.; Schumann, U.; Stoll, H.; Stone, A. J.; Tarroni, R.; Thorsteinsson, T. University College Cardiff: Cardiff, U.K., 2006; see <http://www.molpro.net>.

(22) Core polarization can be important in charged systems. We verified that core polarization does not contribute to the QCISD(T)/CBS relative energies in the reaction path of **1**.

(23) Perdew, J. P.; Burke, K.; Ernzerhof, M. *Phys. Rev. Lett.* **1996**, *77*, 3865–3868.

(24) For example, the VASP program incorporates the PBE functional. See: (a) Kresse, G.; Hafner, J. *Phys. Rev. B* **1993**, *47*, 558–561. (b) Kresse, G.; Hafner, J. *Phys. Rev. B* **1994**, *49*, 14251–14269. (c) Kresse, G.; Furthmüller, J. *Comput. Mater. Sci.* **1996**, *6*, 15–50. (d) Kresse, G.; Furthmüller, J. *Phys. Rev. B* **1996**, *54*, 11169–11186.

(25) The relevance of basis set superposition error (BSSE) was checked by calculating the CBS energies for B3LYP and PBE. BSSE was found to not play an important role in the relative energetics of this isomerization.

(26) These calculations were performed in a manner similar to that described in ref 19, except that the extrapolations were performed using MP2/aug-cc-pVDZ and MP2/aug-cc-pVTZ energies for reasons of economy. For comparative purposes, this extrapolation is sufficient.

(27) As a single example, see: Fărcașiu, D.; Lukinskas, P.; Pamidigantam, S. V. *J. Phys. Chem A* **2002**, *106*, 11672–11675.